Exploration of direct neutron capture with covariant density functional theory inputs

Shi-Sheng Zhang,[1,2,3,*] Jin-Peng Peng,[1] M. S. Smith,[2,†] G. Arbanas,[4] and R. L. Kozub[5]
[1]*School of Physics and Nuclear Energy Engineering, Beihang University, Beijing 100191, China*
[2]*Physics Division, Oak Ridge National Laboratory, Oak Ridge, Tennessee 37831-6354 USA*
[3]*Department of Physics and Astronomy, University of Tennessee, Knoxville, Tennessee 37996, USA*
[4]*Reactor and Nuclear Systems Division, Oak Ridge National Laboratory, Oak Ridge, Tennessee 37831-6171 USA*
[5]*Department of Physics, Tennessee Technological University, Cookeville, Tennessee 38505 USA*
(Received 4 November 2014; revised manuscript received 23 January 2015; published 10 April 2015)

Predictions of direct neutron capture are of vital importance for simulations of nucleosynthesis in supernovae, merging neutron stars, and other astrophysical environments. We calculated direct capture cross sections using nuclear structure information obtained from a covariant density functional theory as input for the FRESCO coupled reaction channels code. We investigated the impact of pairing, spectroscopic factors, and optical potentials on our results to determine a robust method to calculate cross sections of direct neutron capture on exotic nuclei. Our predictions agree reasonably well with experimental cross section data for the closed shell nuclei ^{16}O and ^{48}Ca, and for the exotic nucleus ^{36}S. We then used this approach to calculate the direct neutron capture cross section on the doubly magic unstable nucleus ^{132}Sn which is of interest for the astrophysical r-process.

DOI: 10.1103/PhysRevC.91.045802 PACS number(s): 25.40.Lw, 21.60.Jz, 26.30.Ca, 26.30.Hj

I. INTRODUCTION

More than half of the elements heavier than iron owe their cosmic origin to the rapid neutron capture process (r-process). Here, high temperatures and neutron densities enable sequences of successive neutron captures to form nuclei near the neutron drip line which subsequently decay toward stability as the system expands and cools [1,2]. Core collapse supernovae [3] and merging neutron stars [4] are the two leading sites for the r-process. To simulate the nucleosynthesis occurring in these systems, it is necessary to determine the rates of neutron capture reactions on neutron-rich unstable nuclei. Capture rates on nuclei near closed neutron shells are of particular importance, as they have been shown to significantly influence predicted r-process abundances [5].

In light of the lack of experimental capture cross sections on the thousands of relevant unstable nuclei, theoretical estimates must be utilized to provide the necessary input for r-process simulations. Statistical models are often used for these estimates, wherein an average over the contribution of individual resonances is made [6,7]. To justify this averaging, there must be a sufficiently high ($\sim$10 levels/MeV) level density in the compound nucleus at energies populated by the incident neutron [8]. Rather than requiring information on the location and properties of individual levels for each nuclear species, statistical model calculations utilize parametrized level density formulas. For example, the popular Fermi gas model has a level density parameter proportional to the nuclear mass [9]. Parametrized level information makes the statistical approach well suited for global calculations; in fact, the community has relied on large-scale statistical model calculations for decades to provide the overwhelming majority of neutron capture cross sections for r-process studies [6].

Statistical models are, however, invalid when the number of available states in the compound system is relatively small. This is known to be the case for low mass nuclei and those near closed shells. It is also thought to be the case for nuclei far from stability [10–12]: approaching the neutron drip-line, neutron separation energies decrease as do deformations, leading in both cases to a lower level density. In such cases, the contribution of two other mechanisms may become dominant—capture through individual unbound levels [resonant capture (RC)] and direct electromagnetic transitions to bound levels [direct capture (DC)]. It was shown through a simple analytical model [13] that the DC contribution may dominate the total cross section for nuclei with closed neutron shells or those with a low neutron binding energy.

Global calculations of DC and RC cross sections are very challenging because they require, as input, information (excitation energies, spins, parities, partial and total widths, spectroscopic factors, optical potential) on the individual levels for every nucleus. The development of theoretical tools to predict this level information for unmeasured neutron-rich unstable nuclei is therefore a crucial step towards improving estimates of neutron capture rates for r-process simulations. A recent study [14] used HFB theory to make global predictions of level properties for DC calculations with the TALYS code. In that study, it was found that the $E2$ and $M1$ components are usually negligible with respect to the $E1$ contribution, but that they can dominate the direct capture rate for several hundred midshell nuclei. For simplicity, we consider only $E1$ contributions in our neutron capture cross section calculations for nuclei near closed shells.

Some previous attempts have used relativistic mean field (RMF) theory to provide single particle (s.p.) levels and one-neutron separation energies for calculations of neutron capture cross sections [8,15]. Two features missing in these studies were consideration of pairing correlations and the coupling of bound levels to resonant levels in the continuum. The positive energy single-particle resonant states play a critical role in

*zss76@buaa.edu.cn
†smithms@ornl.gov

the description of exotic nuclei with small binding energies, because valence nucleons can be readily scattered both into bound states above the Fermi surface and into resonant states in the continuum. It is known from previous studies [16,17] that consideration of the coupling and pairing correlations can, in some cases, significantly influence predictions of the location and properties of resonant levels and the neutron capture threshold (i.e., the one neutron separation energy). Therefore, they are crucial for determining the neutron capture cross sections needed for r-process simulations.

II. APPROACH

To address this, we used a microscopic covariant density functional theory based on an RMF approach with contributions from resonant orbitals included via the analytical continuation of the coupling constant (ACCC) approach, and pairing correlations involved by the resonant Bardeen-Cooper-Schrieffer (BCS) approach. This RMF + ACCC + BCS approach [18,19], denoted by RAB for simplicity below, was recently used to describe s.p. levels in unstable nuclei including ^{131,133}Sn [12], and the p-wave halo nucleus ^{31}Ne [16]. In the BCS approximation, a constant pairing strength is determined for each nucleus by fitting the odd-even mass difference extracted from a three-point formula for neutron pairs in a procedure described in detail in Refs. [16,19].

There are several advantages to this covariant density functional RAB approach: self-consistent treatment of resonant levels, auto-inclusion of spin-orbit coupling interactions, use of a relativistic mean field model, and pairing correlations. The RAB approach was developed on the basis of the RMF theory [20], which provides successful *global* calculations of many properties of exotic nuclei [21–23]—including binding energies, charge radii, and energies of bound levels. RMF models typically use only ten interaction parameters that are determined by fits to finite nuclear properties. In this scheme, nuclear structure for nuclei both near and far from β stability can be reasonably well described [12,16,19,24,25].

We applied this microscopic covariant density functional approach to calculate the energies and properties of bound levels in three nuclei which have low level densities, few or no resonances above threshold, and existing experimental capture data: the double closed shell nuclei ^{16}O and ^{48}Ca, and the neutron-rich nucleus ^{36}S. We then used the information for these levels as inputs for the FRESCO reaction code [26] in which radiative capture (direct capture for $E1$ transition) cross sections are obtained by a one-step distorted-wave Born approximation (DWBA) using an energy-dependent optical model potential (OMP) for scattering states [27]. The s.p. level energies, normalized to one-neutron separation energy, are crucial inputs for FRESCO, for which we used three sources: available data [28]; RMF model predictions; and our developed RAB approach [18] with the NL3 effective interactions [29]. The FRESCO code internally optimizes a Woods-Saxon shape potential to reproduce the input bound s.p. level energies. Spectroscopic factors (SFs) are also crucial inputs for our calculations. Generally, theoretical SFs are bigger than those obtained from (d,p) reaction measurements, often approaching the maximal value of 1.0, and we compared cross section predictions when both are available. For scattering states, we used two popular OMPs: Köning-Delaroche (KD) [30] and (for nuclei with mass greater than 40) Chapel Hill (CH89) [31]. To build up a robust procedure, we compared FRESCO cross section predictions using different structure inputs to experimental capture cross section data. This enabled us to determine a preferred approach to predict DC cross sections on exotic nuclei near closed shells for which no capture data σ_γ exist. We then tested our procedure on ^{132}Sn and compared our results to a recent theoretical prediction since there is no σ_γ data for this nucleus.

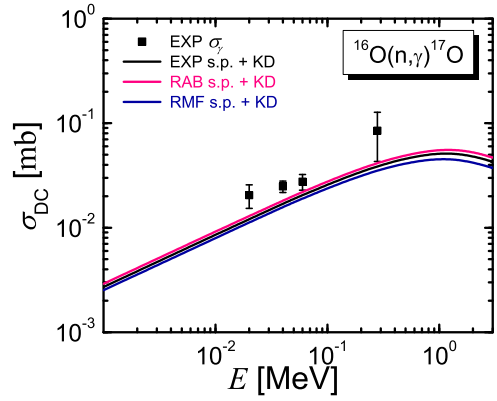

FIG. 1. (Color online) Direct neutron capture cross section σ_{DC} for $^{16}O(n,\gamma)^{17}O$. Full squares: experimentally measured cross section [33]. Pink line: FRESCO calculations with s.p. level energies from RAB approach. Green line: similarly but with RMF s.p. level energy inputs. Black line: similar with experimental level energies. KD optical potentials of scattering states are used with SF = 1.

III. RESULTS AND DISCUSSION

Our calculations for ^{16}O are shown in Fig. 1 over the energy range 10^{-3} MeV to 3 MeV of interest for nuclear astrophysics. Here, we used SFs of 1.0 for incoming p-wave scattering state transitions to the $\frac{5}{2}^+$ or $\frac{1}{2}^+$ s.p. levels [32], and used the KD OMP to describe the scattering states. In our self-consistent RAB calculations, we chose the pairing strength $G = 20$ to reproduce a pairing gap of $\Delta = 2.0$ MeV for ^{17}O, and we determined FRESCO inputs of s.p. level energies and one-neutron separation energies from those s.p. levels within the model. It can be seen from Fig. 1 that our σ_{DC} calculations with the FRESCO code using structure information from RAB and RMF approaches agree within 2σ of experimental data [33]. Similar results are presented in Ref. [14], in which HFB theory is used along with the Bruyères-le-Châtel renormalization of the Jeukenne-Lejeune-Mahaux (JLMB) optical potential. The direct comparison of our predicted σ_{DC} with the experimentally measured cross section σ_γ for ^{16}O is validated by the inapplicability of the statistical model for such low-Z nuclei (see, e.g., [8]).

We also used our approach to study neutron capture cross section on the neutron-rich sulfur isotope ^{36}S. This reaction contributes significantly to the s-process nucleosynthesis in the S-Cl-Ar-Ca region [34], to inhomogeneous Big Bang scenarios [35,36], and to the α-rich freeze-out in core collapse

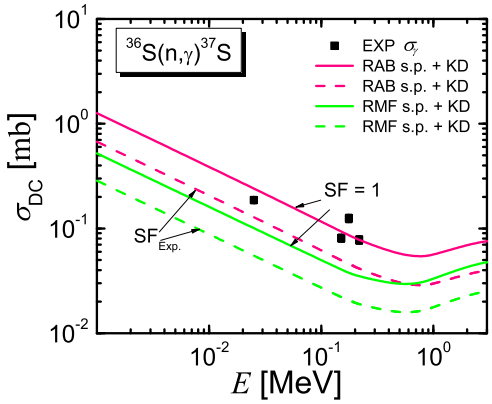

FIG. 2. (Color online) Similar as Fig. 1, but for the ^{36}S$(n,\gamma)^{37}$S reaction. Solid lines refer to the results of the FRESCO code with SF = 1, dashed lines use SF from (d,p) measurements [40]).

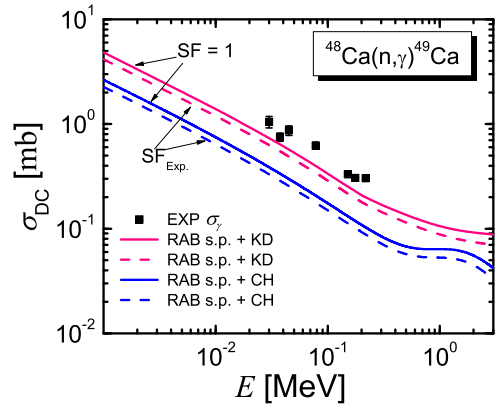

FIG. 3. (Color online) Similar as Fig. 2, but for the ^{48}Ca$(n,\gamma)^{49}$Ca reaction. Blue lines refer to the results with CH89 optical potentials.

supernovae [37–39]. The direct capture cross section on ^{36}S is considered a benchmark of structure model input for calculations of neutron capture on unstable nuclei in the r-process [15,40].

Our σ_{DC} calculations for ^{36}S$(n,\gamma)^{37}$S are displayed in Fig. 2 along with experimental σ_γ data [40]. The pairing strength of $G = 20$ was used to reproduce a pairing gap of $\Delta = 1.2$ MeV for ^{37}S. Here we compared results with theoretical SFs of 1.0 to those with SFs extracted from (d,p) measurements [15]. This figure demonstrates that the calculations with RAB inputs are closer to measured σ_γ [40] than those from RMF inputs. This is likely due to the consideration of resonant states and pairing correlations between positive-energy (resonant) states and negative-energy (bound) states for this exotic nucleus. We surmise that proper descriptions of the pairing correlations and resonant contributions for finite nuclei will help better predict σ_{DC} for other exotic nuclei as well. We note that the cross section enhancement near 198 keV comes from resonant contributions [41] which were not included in our σ_{DC} calculations.

We included direct capture into the $\frac{3}{2}^-$, $\frac{1}{2}^-$, and $\frac{7}{2}^-$ s.p. levels in our RAB calculations; the main contribution to σ_{DC} comes from the $\frac{3}{2}^-$ level, with some additional contribution from the $\frac{1}{2}^-$ level and almost none from the $\frac{7}{2}^-$ level. We calculated the contribution from the statistical Hauser-Feshbach (HF) model over the range of experimentally measured energies. The total cross section—the sum of direct and compound nuclear contributions—agrees well with the experimentally measured values, and is comprised of approximately 60% direct and 40% compound contributions. The corresponding direct capture contributions σ_{DC} mentioned above are calculated with RAB s.p. levels, the KD optical potential, and SFs from (d,p) measurements. We note that the total cross section overpredicts the experimental values if σ_{DC} is calculated with theoretical SFs.

We carried out similar calculations for ^{48}Ca$(n,\gamma)^{49}$Ca, one of the few nuclei in the mass range 36–66 where experimental σ_γ data exist. Knowledge of the cross sections in this mass range is needed to help understand isotopic anomalies of Ca-Al-rich inclusions of certain primitive meteorites [42–44].

Our σ_{DC} calculations are shown in Fig. 3 along with experimental data [28,45]. Since the CH89 OMP was developed for masses greater than 40, we compared FRESCO calculations with CH89 and KD optical model parameters. We used the pairing strength $G = 20$ to reproduce a pairing gap of $\Delta = 0.6$ MeV for ^{49}Ca in our RAB calculations. We also compared results with SF = 1 and with SF extracted from (d,p) measurements [46]. The KD OMP clearly gives better agreement with measured σ_γ than does the CH89 OMP. This is caused by the imaginary part of the CH89 OMP being larger than that in the KD OMP, resulting in a larger absorption and a smaller σ_γ. The predictions with SF = 1 are again closer to measured σ_γ values. From the contributions of each orbital, we find that $E1$ transitions from incoming s-wave scattering state to the $\frac{1}{2}^-$ and $\frac{3}{2}^-$ s.p. levels dominate σ_{DC}, with a significantly smaller contribution for transitions from the d-wave scattering state to the $\frac{5}{2}^-$ s.p. level. We estimated the contribution of the statistical process for neutron capture on ^{48}Ca at these energies and found it to be approximately 10%, validating the direct comparison of our predicted σ_{DC} with the experimentally measured cross section σ_γ for this nucleus.

We then followed the approach described above to calculate σ_{DC} on the unstable nucleus ^{132}Sn relevant for the r-process. The double magic nature of ^{132}Sn was recently determined from the strong s.p. levels (with SFs near 1.0) measured by the ^{132}Sn(d,p) reaction [47]. Since there are no experimental σ_γ data for ^{132}Sn, we compared our predictions to a recent theoretical study of σ_{DC} which determined real potentials for each orbital by fitting the measured s.p. level energies [48]. We first used experimental s.p. level energies and the KD OMP to evaluate σ_{DC} and the components from each orbital with the same assumption of SF = 1 used in Ref. [48]. As clearly shown in Fig. 4, our predictions reasonably agree with those of Ref. [48]. We then used a pairing strength of $G = 12$ to reproduce a pairing gap of $\Delta = 0.3$ MeV for ^{133}Sn in our RAB calculations (Fig. 5). We found that the $E1$ transitions to the $\frac{3}{2}^-$ and $\frac{1}{2}^-$ s.p. levels in ^{133}Sn dominate the capture cross section at low energies. Above 0.7 MeV, the $E1$ transition to

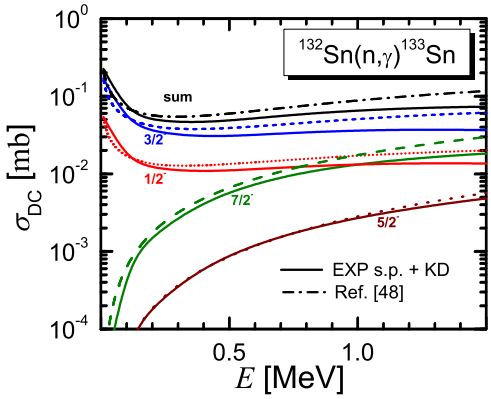

FIG. 4. (Color online) Calculations of direct capture cross sections for ^{132}Sn$(n,\gamma)^{133}$Sn and the individual level contributions. Solid lines: FRESCO calculations with measured s.p. level energy inputs with KD optical potential and SF = 1. Dashed lines: σ_{DC} from Ref. [48].

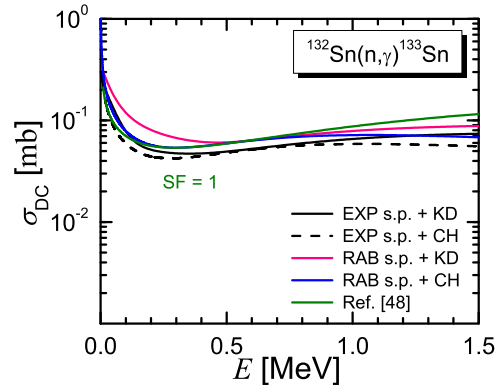

FIG. 5. (Color online) Calculations of direct capture cross sections for ^{132}Sn$(n,\gamma)^{133}$Sn by different approaches with SF = 1. Black solid line: FRESCO calculations with measured s.p. level energy inputs with KD optical potential. Black dashed line: FRESCO calculations with measured s.p. level energy inputs with CH89 optical potential. Pink line: FRESCO calculations with RAB s.p. level energy inputs with KD optical potential. Blue line: FRESCO calculations with RAB s.p. level energy inputs with CH89 optical potential. Green line: σ_{DC} from Ref. [48].

the $\frac{7}{2}^-$ level become comparable with that to the $\frac{1}{2}^-$ level. The predictions of Ref. [48] (nonsolid lines in Fig. 4 and green solid line in Fig. 5) are slightly higher than our predictions with KD OPM, and are likely due to the different potentials for scattering and using different codes for the calculations. To determine the spread of σ_{DC} values for ^{132}Sn$(n,\gamma)^{133}$Sn, we compared predictions using different combinations of energy levels (RAB or experimental) and OMP (KD and CH89); our results are shown in Fig. 5. The trend of the σ_{DC} curves are similar for all cases and the prediction of RAB using KD OMP (pink solid line) lies between the prediction of Ref. [48] and our calculation using experimental s.p. levels with the KD OMP at r-process energies. All predictions give $\sigma_{DC} \approx 0.05$–0.1 mb for ^{132}Sn$(n,\gamma)^{133}$Sn for the neutrons in the energy range relevant for the r-process. The variation of σ_{DC} between the four cases shown in Fig. 5 is less than a factor of two.

IV. SUMMARY

We utilized the FRESCO code with different structure inputs—s.p. levels from measurements and from RMF and RAB calculations—in order to build up a robust procedure to predict σ_{DC} for unstable nuclei near closed neutron shells which are crucial for r-process simulations. We found that for exotic nuclei, pairing correlations significantly change our σ_{DC} predictions, as exemplified by ^{36}S$(n,\gamma)^{37}$S. We also found that the contribution from the direct capture mechanism is comparable to that from the compound nuclear mechanism for this particular exotic nucleus. The KD optical potential, when combined with the covariant density functional RAB approach, gives a better description than does the CH89 optical potential. Our approach gives comparable results to those from a nonrelativistic HFB calculation with the JLMB optical potential [14]. For those nuclei in which s.p. levels are measured from experiments, our FRESCO calculations using existing s.p. level energies and the KD OMP inputs give results that agree reasonably well with the measured σ_γ. The procedure we developed works well for ^{16}O$(n,\gamma)^{17}$O, ^{36}S$(n,\gamma)^{37}$S, and ^{48}Ca$(n,\gamma)^{49}$Ca. Based on this, we recommend using the FRESCO code with RAB s.p. level energies and KD OMP inputs for exotic nuclei where s.p. levels and σ_γ have not been measured. Our future efforts will include the incorporation of resonant capture and the use of a deformed covariant density functional model with resonant contributions and pairing correlations, in order to describe neutron capture reactions on ^{58,62}Ni [49,50] and other exotic Sn isotopes.

ACKNOWLEDGMENTS

This work has been supported by the National Natural Science Foundation of China (Grants No. 11375022 and 11235002), China Scholarship Council (No. 2011307472), Beihang New Star; the U.S. Department of Energy, Office of Science, Office of Nuclear Physics; and the U.S. Dept. of Energy Topical Collaboration in Theory of Reactions on Unstable iSotopes (TORUS) and Chinese U.S Theory Institute for the Physics of Exotic Nuclei (CUSTIPEN). We acknowledge helpful discussions with Prof. I. J. Thompson, Prof. Shan-Gui Zhou, Prof. F. M. Nunes, Dr. A. J. Signoracci and Dr. B. Manning.

[1] B. S. Meyer, Ann. Rev. Astron. Astrophys. **32**, 153 (1994).

[2] S. Goriely, J. L. Sida, J. F. Lemaître *et al.*, Phys. Rev. Lett. **111**, 242502 (2013).

[3] P. Banerjee, Y.-Z. Qian, W. C. Haxton, and A. Heger, Phys. Rev. Lett. **110**, 141101 (2013).
[4] S. Goriely, A. Bauswein, and H. T. Janka, Astrophys. J. Lett. **738**, L32 (2011).
[5] R. Surman and J. Engel, Phys. Rev. C **64**, 035801 (2001).
[6] T. Rauscher and F. K. Thielemann, At. Data Nucl. Data Tables **75**, 1 (2000); **79**, 47 (2001).
[7] S. Goriely, S. Hilaire, and A. J. Köning, Astron. Astrophys. **487**, 767 (2008).
[8] T. Rauscher, F. K. Thielemann, and K. L. Kratz, Phys. Rev. C **56**, 1613 (1997).
[9] A. J. Köning, S. Hilaire, and S. Goriely, Nucl. Phys. A **810**, 13 (2008).
[10] S. Goriely, Astron. Astrophys. **325**, 414 (1997).
[11] A. Mengoni, T. Otsuka, and M. Ishihara, Phys. Rev. C **52**, R2334 (1995).
[12] S. S. Zhang, M. S. Smith, G. Arbanas, and R. L. Kozub, Phys. Rev. C **86**, 032802(R) (2012).
[13] G. J. Mathews, A. Mengoni, F. K. Thielemann, and W. A. Fowler, Astrophys. J. **270**, 740 (1983).
[14] Y. Xu and S. Goriely, Phys. Rev. C **86**, 045801 (2012).
[15] H. Oberhummer, W. Balogh, R. Bieber, H. Herndl, U. Langer, T. Rauscher, and H. Beer, *Proceedings of the International Conference on Exotic Nulcei and Atomic Masses* (ENAM95), Arles, France (Les Editions Frontieres, Gif-surYvette, 1995).
[16] S. S. Zhang, M. S. Smith, Z. S. Kang, and J. Zhao, Phys. Lett. B **730**, 30 (2014).
[17] Y. Zhang, M. Matsuo, and J. Meng, Phys. Rev. C **86**, 054318 (2012).
[18] S. S. Zhang, J. Meng, S. G. Zhou, and G. C. Hillhouse, Phys. Rev. C **70**, 034308 (2004).
[19] S. S. Zhang, Int. J. Mod. Phys. E **18**, 1761 (2009).
[20] P. Ring, Prog. Part. Nucl. Phys. **37**, 193 (1996).
[21] J. Meng and P. Ring, Phys. Rev. Lett. **77**, 3963 (1996); J. Meng, Nucl. Phys. A **635**, 3 (1998).
[22] J. Meng, H. Toki, S. G. Zhou, S. Q. Zhang, W. H. Long, and L. S. Geng, Prog. Part. Nucl. Phys. **57**, 470 (2006).
[23] S. G. Zhou, J. Meng, P. Ring, and E. G. Zhao, Phys. Rev. C **82**, 011301(R) (2010).
[24] S. S. Zhang, X. D. Xu, and J. P. Peng, Eur. Phys. J. A **48**, 40 (2012).
[25] S. S. Zhang, E. G. Zhao, and S. G. Zhou, Eur. Phys. J. A **49**, 77 (2013).
[26] http://www.fresco.org.uk.
[27] I. J. Thompson and F. M. Nunes, *Nuclear Reactions for Astrophysics: Principles, Calculation and Applications of Low-Energy Reactions* (Cambridge University Press, Cambridge, 2009).
[28] http://www.nndc.bnl.gov/.
[29] G. A. Lalazissis, J. König, and P. Ring, Phys. Rev. C **55**, 540 (1997).
[30] A. J. Koning and J. P. Delaroche, Nucl. Phys. A **713**, 231 (2003).
[31] R. L. Varner, W. J. Thompson, T. L. McAbee *et al.*, Phys. Rep. **201**, 57 (1991).
[32] J. T. Huang, C. A. Bertulani, and V. Guimaraes, At. Data Nucl. Data Tables **96**, 824 (2010).
[33] M. Igashira, Y. Nagai, K. Masuda, T. Ohsaki, and H. Kitazawa, Astrophys. J. **441**, L89 (1995).
[34] S. Druyts, C. Wagemans, and P. Geltenbort, Nucl. Phys. A **573**, 291 (1994).
[35] R. Malaney and G. J. Mathews, Phys. Rep. **229**, 145 (1993).
[36] T. Rauscher, J. H. Applegate, J. C. Cowan, F. K. Thielemann, and M. Wiescher, Astrophys. J. **429**, 499 (1994).
[37] S. E. Woosley, J. R. Wilson, G. J. Mathews, R. D. Hoffmann, and B. S. Meyer, Astrophys. J. **433**, 229 (1994).
[38] W. M. Howard, S. Goriely. M. Rayet, and M. Arnould, Astrophys. J. **417**, 713 (1993).
[39] J. Witti, H. T. Janka, and K. Takahashi, Astrophys. J. **286**, 841 (1994).
[40] H. Beer, P. V. Sedyshev, Yu. P. Popov, W. Balogh, H. Herndl, and H. Oberhummer, Phys. Rev. C **52**, 3442 (1995).
[41] P. M. Endt, Nucl. Phys. A **521**, 1 (1990).
[42] D. G. Sandler, S. E. Koonin, and W. A. Fowler, Astrophys. J. **259**, 908 (1982).
[43] W. Ziegert, M. Wiescher, K.-L. Kratz, P. Möller, J. Krumlinde, F.-K. Thielemann, and W. Hillebrandt, Phys. Rev. Lett. **55**, 1935 (1985).
[44] A. Wöhr *et al.*, in *Proceedings of the Eighth International Symposium on Gamma-Ray Spectroscopy and Related Topics*, Fribourg, Switzerland, edited by J. Kern (World Scientific, Singapore, 1994), p. 762.
[45] H. Beer, C. Coceva, P. V. Sedyshev, Yu. P. Popov, H. Herndl, R. Hofinger, P. Mohr, and H. Oberhummer, Phys. Rev. C **54**, 2014 (1996).
[46] Y. Uozumi, O. Iwamoto, S. Widodo, A. Nohtomi, T. Sakae, M. Matoba, M. Nakano, T. Maki, and N. Koori, Nucl. Phys. A **576**, 123 (1994).
[47] K. L. Jones *et al.*, Nature **465**, 454 (2010); Phys. Rev. C **84**, 034601 (2011).
[48] P. Mohr, Phys. Rev. C **86**, 068803 (2012).
[49] P. Zugec *et al.*, Phys. Rev. C **89**, 014605 (2014).
[50] C. Lederer *et al.*, Phys. Rev. C **89**, 025810 (2014).